# Current Assessment Methodology for Electrostatic Discharge Hazards of Energetic Materials

J. Covino* and F. E. Hudson†
*Naval Weapons Center, China Lake, California 93555*

**The 1985 Pershing fire and other more recent incidents have renewed interest in the phenomenon of electrostatic discharge (ESD) in energetic materials as a mechanism for induced inadvertent ignition and sustained combustion. In recent years, ESD research has focused on developing experimental techniques to evaluate ESD hazards of energetic materials. In this paper, logic/protocol is described for assessing ESD sensitivity in energetic materials consisting of a calculation percolation coefficient and measurements of resistivity, dielectric constant, dielectric breakdown, and resistive-capacitive (R-C) discharge. Representative data on energetic and nonenergetic propellant formulations are presented and discussed.**

## Nomenclature

| | |
|---|---|
| $d_{cf}$ | = diameter of finest fraction of conducting particles |
| $d_{nf}$ | = diameter of finest fraction of nonconducting particles |
| vol%$b$ | = volume percent of binder |
| vol%$C$ | = volume percent of conducting particles |
| vol%$nf$ | = volume percent of finest fraction of nonconducting particles |
| wt%$b$ | = weight percent of the binder |
| wt%$C$ | = weight percent of conducting particles |
| wt%$n$ | = weight percent of all nonconducting particles |
| wt%$nf$ | = weight percent of finest fraction of nonconducting particles |
| $\rho_b$ | = density of the binder |
| $\rho_c$ | = density of conducting particles |
| $\rho_n$ | = density of nonconducting particles |
| $\rho_{vb}$ | = volume resistivity of the binder, Ω·m |

## Introduction

ON January 11, 1985, in Heilbron, Germany, a Pershing II missile with a Kevlar-cased rocket motor containing an aluminized hydroxyl-terminated polybutadiene (HTPB) propellant ignited, killing three people.[1,2] The subsequent investigation suggested that motor ignition could be attributed to electrostatic discharge (ESD) through the motor following the separation of dissimilar dielectric materials in a cold, dry climate. These findings prompted the propulsion community to study the ESD hazard of solid rocket propellants.

Static charge can be generated by several means: 1) *Triboelectric effects* result when a nonconductive surface first contacts and then is separated from a second surface; 2) *Polarization* causes materials to acquire a static charge when under the influence of an electric field; 3) *Thermionic emission* is emission of electrons caused by raising the particle temperature; 4) *Photoelectric charging* where light quanta imparts sufficient energy to eject electrons from the surface; 5) *Radioactive decay* where, if a particle is composed of material containing a beta emitter, for example, an isolated particle will be charged to the energy at which local breakdown of the surrounding atmosphere takes place or, alternatively, until field emission of positive ions occurs from particle asperities; 6) *Mechanical fracture* where the mechanism proposed for the generation of electrons is that of emission from ruptured, strained, or otherwise mechanically broken bonds within solids; and 7) *Charging by freezing* where potential differences that are induced during the freezing process, e.g., during the freezing of water. Through these mechanisms, a considerable electrostatic charge can be created during the handling and manufacturing of a solid rocket motor. For example, recorded electric potentials on a propellant core may exceed several thousand volts at the end of a mandrel pullout operation. Rocket motor manufacturers and government facilities have extensively implemented preventive measures efficient for reducing charge accumulation. These measures include the use of graphite (both as a propellant ingredient and as graphite composite motor cases) and of systematic grounding. Since preventive operations cannot provide an absolute warranty against the occurrence of all hazardous events, it is important to understand the behavior and sensitivity of propellants (specifically composite propellants) to ESD.

A severe hazard arises when energetic materials used in ammunition and propulsion systems are charged to a potential where breakdown occurs, or when a change in grounding conditions allows breakdown of the material. Discharge processes generate charge carriers, which reduce the impedance of the energetic material and result in a rapid current increase. This can lead to arcing, establishment and growth of discharge paths, followed by catastrophic discharge. The resulting pressure and temperature increase in the very narrow discharge path and may induce ignition and combustion.

Before the Pershing incident, ESD sensitivity levels of rocket motor propellants were determined by capacitive discharge. This test method had been in use for many years and is based on experimental work performed by the U.S. Bureau of Mines,[3] but a detailed methodology has not been standardized and differs between government agencies and propellant manufacturers. In general, a voltage source charges a capacitor through a resistor, which is then connected to the test sample. The energetic material, usually in the form of a powder, is placed in a cup that completes the electrical circuit. The sample size is small to minimize the effect of the reaction. A probe is moved toward the sample until an arc discharge occurs. The capacitance $C$ and resistance $R$ are adjusted until a reaction occurs and the stored energy is calculated as an indication of sensitivity.

The Pershing incident established that a propellant that would be considered insensitive to ESD at 70°F could in fact be sensitive at a lower temperature. This observation compels the retesting of existing, fielded propellants at other temperatures.

Received July 23, 1989; revision received Oct. 5, 1989; accepted for publication April 23, 1990. 

*Research Chemist, Code 3891.
†Electronic Technician, Code 3891.

**Table 1 Inert propellant formulations[a]**

| Sample | Weight % | | | | Volume % | | | |
|---|---|---|---|---|---|---|---|---|
| | 3 μm aluminum | Coarse NaCl, ~550 μm | Fine NaCl, ~150–200 μm | Total NaCl | 3 mm aluminum | Coarse NaCl, ~550 μm | Fine NaCl, ~150–200 μm | Total NaCl |
| KJ-17 | 5 | 37.2 | 37.8 | 75 | 2.978 | 28.094 | 27.6485 | 55.743 |
| KJ-14 | 20 | 37.2 | 22.8 | 60 | 12.699 | 29.481 | 18.069 | 47.545 |
| KJ-15 | 35 | 37.2 | 7.8 | 45 | 22.414 | 29.732 | 6.234 | 35.966 |
| KJ-16 | 50 | 30.0 | 0 | 30 | 33.376 | 24.993 | 0 | 24.993 |
| KJ-18 | 80 | 0 | 0 | 0 | 54.692 | 0 | 0 | 0 |

[a]All propellants contain 20 wt% HTPB as binder. Density in g/cc: aluminum = 2.702, NaCl = 2.165, binder = 0.93, binder volume resistivity = $3 \times 10^{10}$ Ω·m.

To assess the ESD sensitivity of munitions, a logic/protocol for propellant testing has been developed at the Naval Weapons Center (NWC). This protocol is based on preliminary work on ESD of propellants performed at the Societé Nationale Des Poudres et Explosifs (SNPE) by Kent and Rat.[4] The logic/protocol was employed both on inert formulations and real propellants, allowing validation for inert samples with predictive extension to energetic materials. This paper attempts to correlate the chemical composition of inert and energetic formulations with electrical properties, and thus ESD sensitivity.

## Experimental Method

### Protocol Methodology for Testing

Figure 1 shows the five steps in the protocol methodology. When evaluating any propellant for ESD sensitivity, all five steps of the protocol testing must be performed. By using this procedure, the ESD sensitivity of propellants currently in use can be evaluated, enabling ranking of propellants in terms of ESD sensitivity. Presently, attempts are being made to understand the ESD phenomena by looking at the propellant ingredients as the electrical building blocks of the propellant. These studies will enable identification of some of the basic parameters necessary to assess the propensity of propellants to ignite upon ESD. It is expected that such data will also enable modeling of the ESD phenomena in propellants and provide a predictive tool for assessing the sensitivity of future propellant formulations. Details of the protocol follow.

### Step 1. Percolation Calculations

In an attempt to understand why certain propellants were ESD sensitive and others were not, Kent and Rat[4] used the percolation theory.[5–7] Factorial examination of propellant active ingredients shows that the aluminum particle size and the

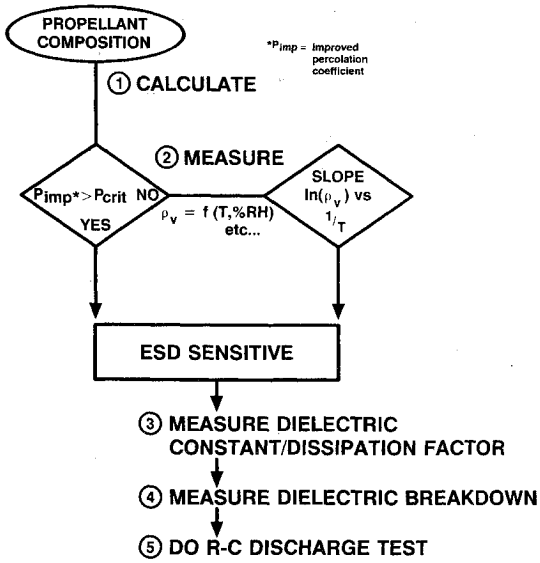


**Fig. 1 Propellant ESD sensitivity logic/protocol.**

**Table 2 Energetic propellant formulations**

| Propellant[a] | Conducting materials | | Wt% of total nonconducting solids (ammonium perchlorate) |
|---|---|---|---|
| | Material | Wt% | |
| A | Aluminum | ~18–20 | ~65–70[b] |
| B | Aluminum | ~18–20 | ~65–70[b] |
| C | ZrC | ~ 1–4 | —— |
| Pershing II, first stage | Aluminum | ~18–20 | ~65–70 |

[a]All propellants contain 10–15 wt% HTPB as the binder.
[b]Propellants A and B have modal distribution of the AP.

electrical properties of the binder (binder = prepolymer + various additives) are major factors in determining that propellant's electrical properties. Kent and Rat[4] found that, at a constant aluminum concentration, as the particle size decreases (i.e., the number of aluminum particles increases) the propellant sensitivity to capacitive discharge increases.

Percolation, as theoretically defined, is independent of the applied voltage and (for a given conducting $N_c$ and insulating $N_i$ particle system) allows determination of a critical ratio between conducting and nonconducting particles ($N_c/N_i$), above which the entire system is fully conducting. In the case of a composite propellant, it does not seem possible to obtain such a level exactly, because the thin oxide covering on the aluminum particle is insulating, while the inner aluminum core is conductive. Nevertheless, all of the aluminum is assumed to be conductive in the percolation calculation.

Recently, Kent and Rat[4] adopted a refined "$P$ breakdown percolation" coefficient equation that seems to be more discriminating. This improved coefficient is defined as

$$P_{\text{imp}} = \left(\frac{\rho_n}{\rho_c}\right)\left(\frac{\text{wt\%}C}{\text{wt\%}nf}\right)\left(\frac{d_{nf}}{d_{cf}}\right)^3\left[\frac{\rho_b}{\text{wt\%}b}\left(\frac{\text{wt\%}C}{\rho_c} + \frac{\text{wt\%}n}{\rho_n}\right) + 1\right]\rho_{vb} = \left(\frac{\text{vol\%}C}{\text{vol\%}nf}\right)\left(\frac{d_{nf}}{d_{cf}}\right)^3\left(\frac{1}{\text{vol\%}b}\right)\rho_{vb} \quad (1)$$

By experimental study, it was found that if $P_{\text{imp}}$ was greater than a threshold value $P_{\text{crit}}$ of $10^{10}$ Ω·m, the propellant was considered potentially hazardous to ESD.

Percolation calculations were performed for five inert propellant formulations shown in Table 1 and the four energetic formulations shown in Table 2. The energetic propellants all contain ammonium perchlorate (AP) as the nonconducting solid (oxidizer), while the inert propellants contain NaCl. The percolation values are tabulated in Table 3 for both inert and energetic formulations.

From the percolation values, one can rank the sensitivity of the inert propellants from least to most sensitive: KJ-17, KJ-14, KJ-15, and KJ-16. KJ-18 cannot be considered because it contains only aluminum particles, thus a percolation value cannot be calculated. The ranking of these inert propellants is directly related to the aluminum concentration. For sample KJ-16, the $P_{\text{imp}}$ value is higher than other samples. This higher value results from the coarse (550 μm) NaCl that was used for the finest fraction of nonconducting particles in the calculation.

One can also rank the energetic formulations, propellant C, propellant B, Pershing II first stage, and propellant A. The $P_{imp}$ value for propellant C has a wide distribution, because the propellant contains variable amounts of ZrC (actually a semiconductor) as the conducting particles.

The percolation breakdown coefficient calculation does not include many critical propellant parameters and cannot fully describe the propellant system accurately. Among these parameters are 1) the highly resistive oxide coating on aluminum particles, and 2) nonspherical particle shapes. Additionally, $P_{crit}$ has been determined simply by experimental results. There is not yet a physical interpretation of why the breakdown coefficient $P_{crit}$ $10^9$ is now $10^{10}$ Ω·m. Furthermore, today's solid rocket propellants are quite complex. For example, they might contain two or more nonconducting species, i.e., AP and AN (ammonium nitrate), which have fine particles, and thus have different contributions to the percent of nonconducting particles. In the percolation equation, all of the nonconducting particles are lumped together, except for the finest fraction of nonconducting particles. Conducting species can also be of a different nature and thus have different chemical and physical properties. For example, both aluminum and carbon, which are highly conductive, are common propellant additives. However, in the percolation equation, all of the conducting species are treated uniformly. Lastly, the binder itself is a complex network, having chemical species with different chemical properties. However, it too is treated as one entity in the percolation calculation. In the percolation equation, $\rho_{vb}$ (volume resistivity of the binder) is a term greatly influencing the $P$ factor. This term is measured experimentally, is temperature, humidity, and time dependent, and thus prone to experimental inconsistencies. In the $P$ calculations presented in this paper, the binder resistivity value used was taken after 30 min, as suggested by Kent and Rat.[4]

**Table 3 $P_{imp}$ values**

| Wt% of 3-μm aluminum | Sample | $P_{imp}$, Ω·m |
|---|---|---|
| Inert propellant samples | | |
| 5 | KJ-17 | $1.4\times10^{13}$ |
| 20 | KJ-14 | $8.8\times10^{13}$ |
| 35 | KJ-15 | $4.4\times10^{14}$ |
| 50 | KJ-16 | $1.6\times10^{17}$ (contains only coarse NaCl) |
| 80 | KJ-18 | Contains only aluminum particles |
| Energetic propellant samples[a] | | |
| A | | $129\times10^{10}$ |
| B | | $20.6\times10^{10}$ |
| C | | $5\times10^{10}$–$8\times10^{8}$ |
| Pershing II, first stage | | $64\times10^{10}$ |

[a]The modal distribution of the AP causes the large energetic differences shown.

### Step 2. Resistivity Measurements

Kent and Rat's[4] experiments suggest that the temperature behavior of a propellant's volume resistivity may be important in the ESD sensitivity of a propellant. They found that propellant volume resistivity measurements from −40 to +80°C (−40 to +176°F) could follow one of three different laws as reflected by a change of slope on a plot of $n$ ($\rho_v$) vs $1/T$ (see Fig. 2). Based on semiconductor theory, the existence of two straight intersecting lines points to a change in the type of conduction. They observed that the compositions that react to capacitive discharges follow a type I or a type II behavior (i.e., the ratio of slopes $M_1/M_2 \geq 1$). However, those that do not react follow a type III behavior (i.e., the ratio $M_1/M_2 < 1$).

Using specially constructed instrumentation, the volume resistivity was measured for the HTPB binder, inert propellant samples, and energetic propellant samples as a function of temperature, time of voltage application, voltage, relative humidity, and sample thickness. Temperatures ranging from −30 to 100°C (−34.4 to 212°F) were achieved with a Tenney Jr. temperature and humidity chamber. Volume resistances of propellant samples were measured on either copper or stainless steel electrodes. Volume resistance was calculated by dividing the applied voltage by the measured current. A Keithley model 617 digital electrometer capable of reading $10^{-15}$ A was used to make the current measurements. Applied voltages ranged from 25–2000 V. Details on measurement techniques and methodology can be found in Refs. 8–11. In this study, data are presented for samples having thickness of 0.6 cm (0.25 in.), a relative humidity of less than 30%, and at an applied voltage of 100 V after 5 min (inert samples) or 4 min (HTPB binder and the energetic samples). Since volume resis-

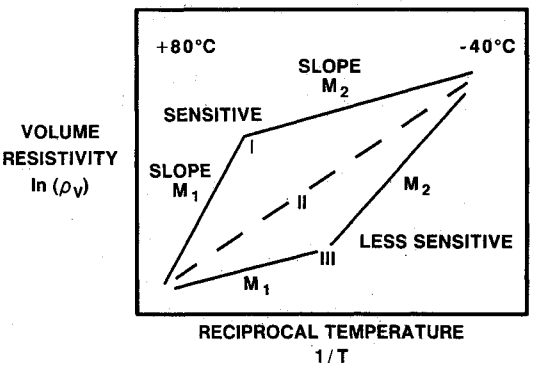


**Fig. 2 Plot of the $\ell n$ ($\rho v$) vs $1/T$ showing the three types of behavior.**

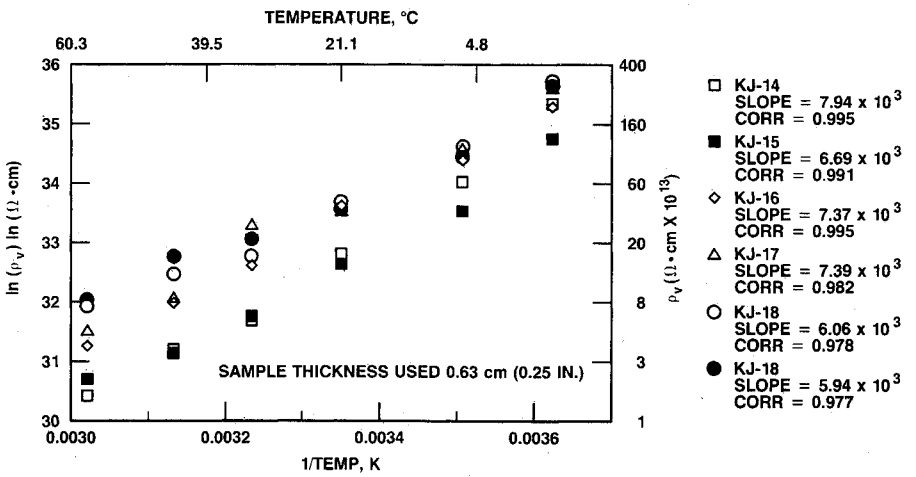


**Fig. 3 Volume resistivity vs temperature for inert propellant samples. Data were taken at 100 V after 5 min and humidities <30%.**

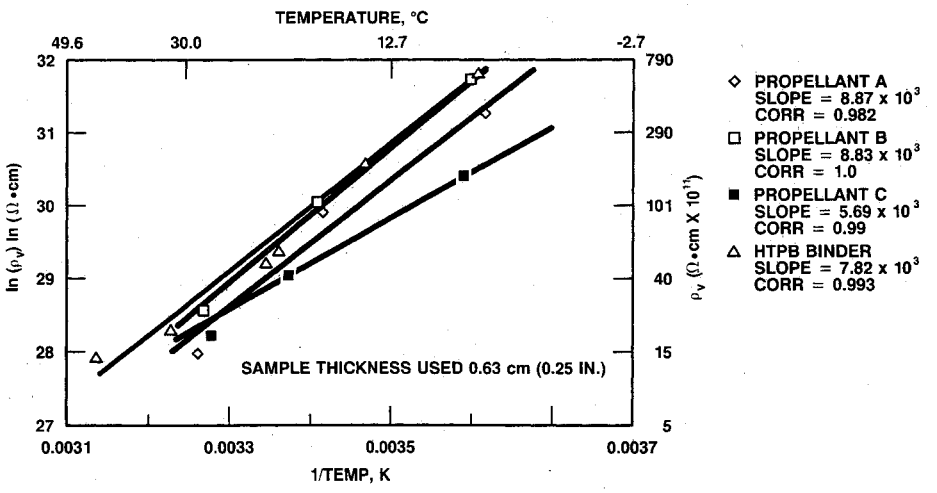


**Fig. 4 Volume resistivity vs temperature for HTPB binder and energetic propellant samples. Data were taken at 100 V after 4 min and at humidities <30%.**

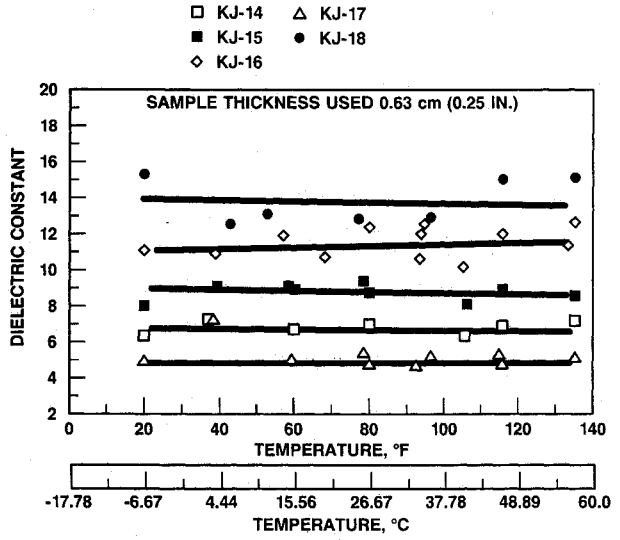


**Fig. 5 Dielectric constant vs temperature for inert propellant samples. Data were taken at 1 kHz and at relative humidities of <30%.**

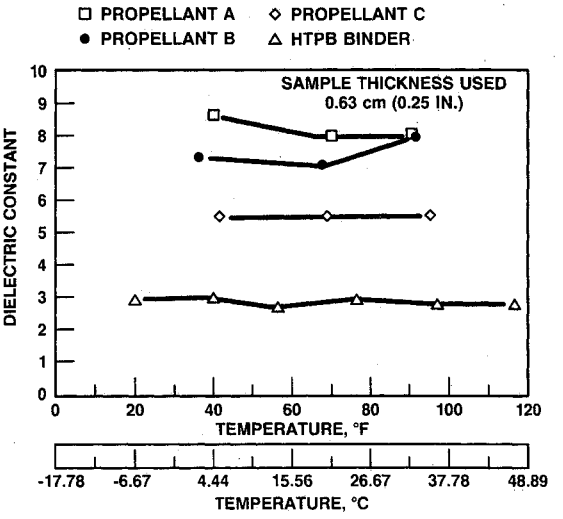


**Fig. 6 Dielectric constant vs temperature for the HTPB binder and energetic propellant samples. Data were taken at 1 kHz and relative humidity <30%.**

tivity is a function of time, the times in the graph were selected only to represent the data in a common, simple fashion for data comparison. In evaluating volume resistivity, all parameters are varied and data evaluated accordingly.

The volume resistivity vs temperature data for the inert samples are summarized in Fig. 3 and show the volume resistivity decreases as the temperature increases. Note that two different KJ-18 samples of different thickness are reported in Fig. 3. Data for the HTPB binder and the energetic samples are shown in Fig. 4. Again the volume resistivity decreases as the temperature increases. Furthermore, it should be observed that the activation energy (slope) for the energetic propellants varies from $5.69 \times 10^3$ $\ell n$ ($\Omega$-cm) K for propellant C to $8.87 \times 10^3$ $\ell n$ ($\Omega$-cm) K for propellant A. Such a significant variation is most likely related to the type, as well as amount, of conducting species within the specific formulation. Since these data show no slope breaks, it can be concluded that these materials all show type II behavior. From the volume resistivity data, one would rank the materials' ESD sensitivity differently than that obtained from percolation calculation data. This difference cannot be explained.

### Step 3. Dielectric-Constant Measurements

The dielectric constant of propellants and propellant ingredients as a function of frequency, temperature, and relative humidity is an important material property that characterizes the energy storage capability and energy discharge potential of the propellant.

Dielectric properties may be measured using a parallel plate capacitor. For details on dielectric theory and measurement techniques, see Refs. 11–15. When making dielectric-constant measurements, a second measurement, the dielectric dissipation factor (loss tangent $D$), is made simultaneously. The dissipation factor is the ratio between the permittivity (dielectric constant) and conductivity of a dielectric (sample). The reciprocal of the dissipation factor is the storage factor, sometimes called the quality factor $Q$.

In this work, the dielectric constant was measured as a function of temperature, relative humidity, sample thickness, and frequency for inert propellants, HTPB binder, and energetic propellants. These data were taken at 1 kHz and are representative of the similarities and differences between the samples. The dielectric constants for the inert propellants are plotted in Fig. 5. These dielectric constants (except for KJ-18) are virtually temperature independent. Figure 6 is a plot of the average dielectric-constant data (each point is the average of three measurements) for the HTPB binder and the energetic propellant samples. The dielectric constants for the HTPB binder and propellant C are temperature independent. The dielectric constant for propellant A ranges from 8.0 to 8.7 and for propellant B from 7.0 to 8.0. For the inert propellant samples, the dielectric constant increases linearly with the

aluminum concentration (see Fig. 7). This increase implies that the dielectric constant is mostly affected by the aluminum concentration. In general, the more aluminum in a propellant formulation, the higher the dielectric constant and the more ESD sensitive the propellant is expected to be. However, the behavior of the dielectric constant with respect to NaCl concentration is more complex. As seen in Fig. 7, the dielectric constant decreases as the volume percent of fine NaCl increases. The behavior of the dielectric constant with total volume percent of NaCl changes little for the first 20% and then decreases linearly with respect to concentration. This result suggests the lowest propellant dielectric constant observed is a consequence of the lowest concentration of conducting particles. It should be noted that when comparing the d.c. data in Fig. 4 with the data at 1 kHz in Fig. 6, the inert propellants do not rank in the same order. The volume resistivity data for the inert propellants do not rank the sample with aluminum concentration. Such an anomaly is not easily explained.

Neglecting the effects of breakdown voltage, the higher the dielectric constant, the more energy can be stored in a material. In this case, the amount of energy that these inert and energetic propellant samples can store is directly proportional to the aluminum concentration and inversely proportional to the NaCl concentration for the inert samples and to the AP concentration for the energetic samples.

Figure 8 illustrates the dependence of the dissipation factor on temperature for the inert samples. As the temperature decreases, the dissipation factor increases. Figure 9 illustrates the temperature dependence of the dissipation factor for the HTPB binder and the energetic propellant samples. The dissipation factor is very small for the HTPB binder (Fig. 9) and exhibits a complicated temperature dependence. The dissipation factor for propellant A is temperature independent, but for propellants B and C increases as the temperature decreases. From the dissipation-factor data, some understanding can be gained of how well and for how long the material can hold a given charge. The larger the dissipation factor, the less likely it is for that material to hold a charge. At lower temperatures, the easier it is for all these materials (except for the HTPB binder and propellant A) to lose or dissipate the applied charge. A comparison of the magnitude of the dissipation factors of the inert propellant samples with that of the HTPB binder and energetic propellants shows that the energetic propellants have much smaller dissipation-factor values. This implies that the energetic propellants can store energy for a longer period of time compared to the inert propellant samples.

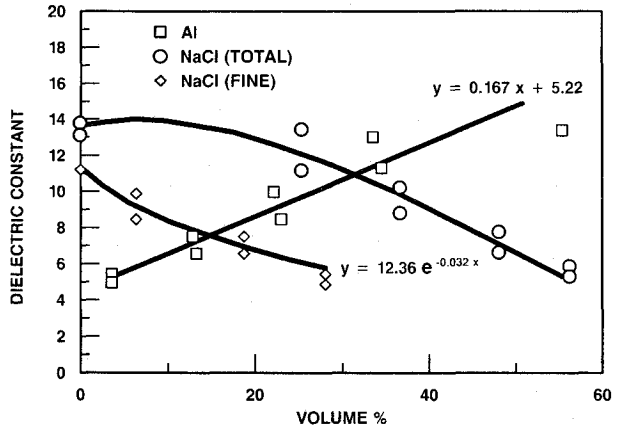


**Fig. 7 Average dielectric constant vs formulation for inert propellant samples.**

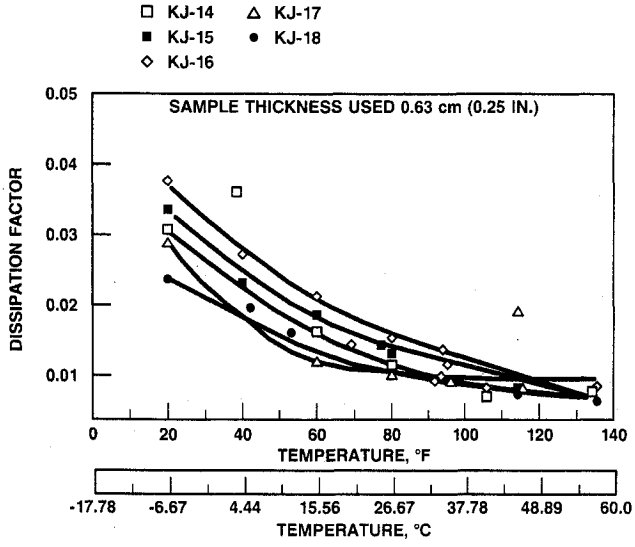


**Fig. 8 Dissipation factor vs temperature for inert propellant samples. Data were taken at 1 kHz and at relative humidities <30%.**

#### Step 4. Dielectric Breakdown

The dielectric-breakdown voltage of a material is the voltage that may be sustained across the sample just prior to transition of the sample from a dielectric material (nonconductive) to a conductor. This breakdown voltage is important in understanding the behavior of the material in an ESD event. The dielectric strength of a material is the dielectric-breakdown voltage divided by the thickness and is measured by following the ASTM D149 procedure.[16-20]

Any of four methods of applying a test voltage may be used in determining the dielectric-breakdown voltage of a material[16]: 1) ramped voltage, 2) stepped voltage, 3) switched capacitor, and 4) pulsed-transformer methods (a coil method developed at NWC). Figure 10 shows the test setup used in all four methods. The measurement can be performed as a function of temperature and relative humidity. During the dielectric breakdown, the applied voltage on the sample and current going through the sample are measured. More details on the theory and experimental methods can be found in Refs. 16–20.

During the ramped voltage tests, the applied voltage is increased in a smooth linear fashion at a rate that will cause breakdown within 20 s. A slow ramp can be a stepped voltage test, which is accomplished by increasing the applied voltage in discrete increments; a variation of this test is to disconnect the sample from the voltage source before each increment.

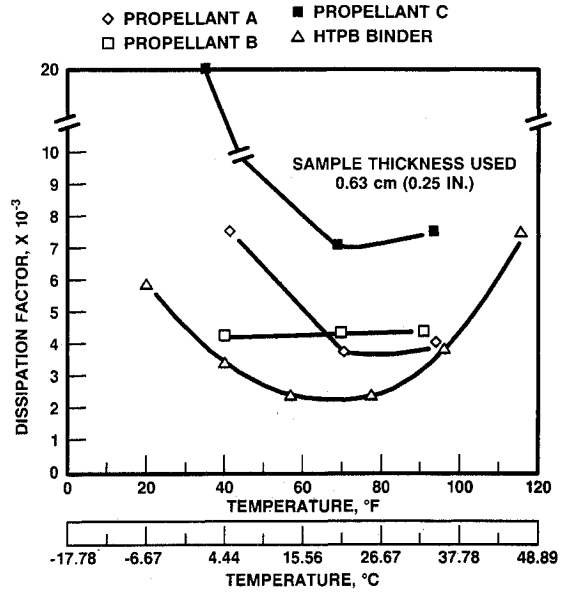


**Fig. 9 Dissipation factor vs temperature for the HTPB binder and energetic propellant samples. Data were taken at 1 kHz.**

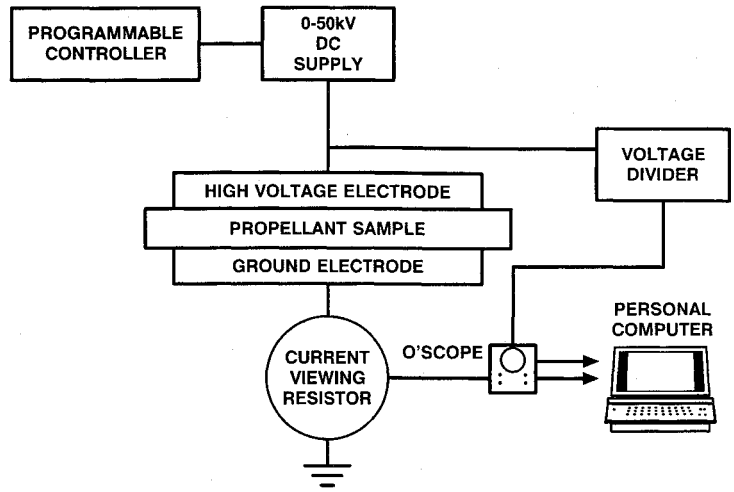


**Fig. 10 Dielectric-breakdown measurement circuit.**

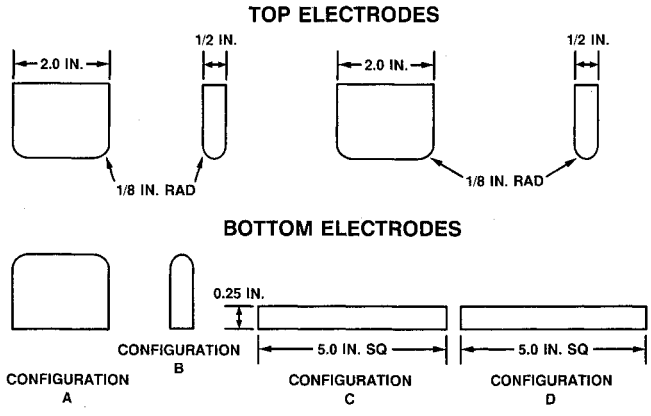


**Fig. 11 The four different electrode configurations used for dielectric-breakdown measurements.**

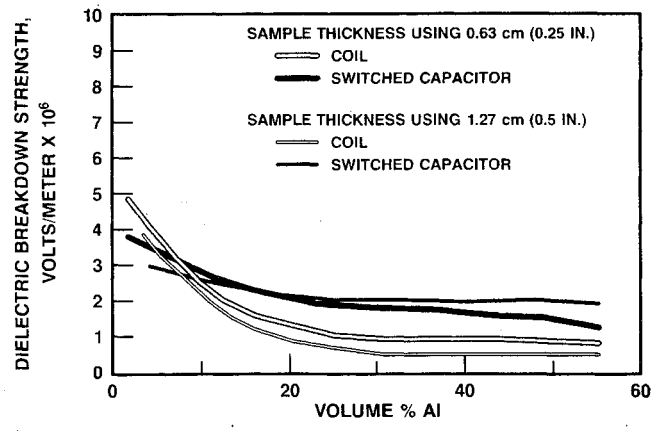


**Fig. 12 Dielectric strength of inert propellants vs volume percent aluminum.**

The switched capacitor test is conducted by charging, then discharging, a capacitor into the sample. The pulsed-transformer method uses a high-voltage pulse as excitation to the sample being tested. The pulse is generated by discharging a capacitor into the primary winding of a high-voltage transformer whose secondary winding is connected to the sample being tested. When the pulse amplitude reaches the breakdown voltage of the sample being tested, loading effects limit any further increase in amplitude. The pulse is clipped at the breakdown voltage of the sample, and the clipping level is easily measured from oscilloscope traces of the pulse waveform.

Unlike the ramped voltage test, the pulsed-transformer (coil) method can be used to test low-resistance samples because the pulse duration is short enough to prevent ohmic heating of the sample. The pulse shape is such that the voltage waveform at the sample is generally free from overshoot and other artifacts observed during switched-capacitor and stepped-voltage tests. Pulsed-transformer testing can also provide data about prebreakdown and postbreakdown characteristics of the sample. For instance, voltage pulses applied to materials that have low breakdown resistance have a much different wave shape than pulses developed on materials with high breakdown resistance. Details of the measurements can be found in Refs. 17 and 18.

Dielectric-breakdown measurements are typically used to establish the voltage at which a material will no longer electrically insulate. Many propellants are too conductive to be considered a dielectric. In these cases, the tests quantify the conditions required for transition from an initial more-resistive state to a less-resistive state. Actual rupture or decomposition of material is positive evidence of voltage breakdown. When neither of these physical evidences of breakdown is apparent, it is common practice to reapply the voltage, which in most cases, will give a positive indication.

Dielectric-breakdown data and dielectric-breakdown field strength were measured for all inert samples as a function of electrode configuration, method of voltage application, and temperature. The breakdown voltage was measured at 17, 79, and 116°F for sample thicknesses of 0.63 and 1.27 cm for the inert samples. In the case of the energetic propellant samples, the dielectric-breakdown voltage was measured at 40, 70, and 90 or 95°F for sample thicknesses of 0.63 and 1.27 cm. These data were taken using the coil method, the switched capacitor method, and the ramp method for the four different electrode configurations shown in Fig. 11.

Tables 4 and 5 summarize the dielectric-breakdown data for the inert propellants. The data were taken using two or more different samples for each temperature. These data showed no temperature dependence for the breakdown field strength. Figure 12 shows that the dielectric strengths of these inert propellants decrease with increasing volume percent of aluminum for all voltage application methods and electrode configurations. The measured dielectric strength of pure 3-$\mu$m aluminum was $0.47 \times 10^6$ V/m,[14] which suggests that aluminum, although the major contributor to dielectric strength, is not the only contributor. The effect of NaCl (AP in real propellants) on breakdown strength is mainly geometrical rather than electrical. The NaCl particle sizes affect the aluminum particle spacing, which is directly related to the dielectric-breakdown voltage. This observation is substantiated by the work of Gibson et al.,[20] who showed that the ESD sensitivity

**Table 4 Dielectric-strength data taken with NWC coil circuit**

| Electrode configuration | Wt% of 3-$\mu$m aluminum | Sample | Temperature/RH | Dielectric strength $\times 10^6$ V/m 0.63-cm sample | 1.27-cm sample |
|---|---|---|---|---|---|
| | 5 | KJ-17 | | 4.70 | 3.63–3.69 |
| | 20 | KJ-14 | 17°F (−8.3°C) | 1.50–1.84 | 1.29 |
| A | 35 | KJ-15 | 14% | 0.65–0.85 | 0.24–0.31 |
| | 50 | KJ-16 | | 0.39–0.52 | 0.28–0.32 |
| | 80 | KJ-18 | | 0.20–0.28 | |
| | 5 | KJ-17 | | 6.61 | 3.79 |
| | 20 | KJ-14 | 79°F (26.11°C) | 2.34–2.53 | 1.93–2.02 |
| A | 35 | KJ-15 | 10% | 1.55–1.73 | 0.80 |
| | 50 | KJ-16 | | 0.68–0.77 | 0.36–0.40 |
| | 80 | KJ-18 | | 0.82 | |
| | 5 | KJ-17 | | 2.38–2.57 | |
| | 20 | KJ-14 | 116°F (46.67°C) | 2.25–2.31 | 1.81–2.1 |
| A | 35 | KJ-15 | 10% | 1.70–1.67 | 0.78 |
| | 50 | KJ-16 | | 1.03 | |
| | 80 | KJ-18 | | | |
| | 5 | KJ-17 | | 2.04–2.57 | |
| | 20 | KJ-14 | 17°F (−8.3°C) | 2.03–2.28 | 0.96–1.07 |
| B | 35 | KJ-15 | 14% | | |
| | 50 | KJ-16 | | | |
| | 80 | KJ-18 | | | |
| | 5 | KJ-17 | | 3.18 | 3.85 |
| | 20 | KJ-14 | 79°F (26.11°C) | 2.07–2.25 | 1.20–1.35 |
| B | 35 | KJ-15 | 10% | | |
| | 50 | KJ-16 | | 0.95 | 0.43–0.51 |
| | 80 | KJ-18 | | 0.92 | |
| | 5 | KJ-17 | | 2.38 | |
| | 20 | KJ-14 | 116°F (46.67°C) | 2.31–2.25 | 1.81 |
| B | 35 | KJ-15 | 10% | 1.67–1.70 | 2.09 |
| | 50 | KJ-16 | | 1.03 | 0.78 |
| | 80 | KJ-18 | | 2.57 | |

**Table 5 Dielectric-strength data taken with the switched capacitor circuit**

| Electrode configuration | Wt% of 3-$\mu$m aluminum | Sample | Temperature/RH | Dielectric strength $\times 10^6$ V/m 0.63-cm sample | 1.27-cm sample |
|---|---|---|---|---|---|
| | 5 | KJ-17 | | 3.92 | 3.21 |
| | 20 | KJ-14 | 17°F (−8.3°C) | 2.18 | 1.32 |
| A | 35 | KJ-15 | 14% | 0.63 | 1.18–2.21 |
| | 50 | KJ-16 | | 1.25 | 1.49–1.57 |
| | 80 | KJ-18 | | 0.62 | |
| | 5 | KJ-17 | | 3.59 | 2.70 |
| | 20 | KJ-14 | 79°F (26.11°C) | 1.98 | 1.71 |
| A | 35 | KJ-15 | 10% | 1.70 | 1.49 |
| | 50 | KJ-16 | | 1.55 | 1.40 |
| | 80 | KJ-18 | | | 0.82 |
| | 5 | KJ-17 | | 3.60 | 2.66 |
| | 20 | KJ-14 | 116°F (46.67°C) | 2.15 | 1.82 |
| A | 35 | KJ-15 | 10% | 1.64 | 1.00–1.68 |
| | 50 | KJ-16 | | 1.36 | 1.48 |
| | 80 | KJ-18 | | | |
| | 5 | KJ-17 | | 1.72–1.88 | |
| | 20 | KJ-14 | 17°F (−8.3°C) | 2.03 | 0.96–1.07 |
| B | 35 | KJ-15 | 14% | | |
| | 50 | KJ-16 | | | |
| | 80 | KJ-18 | | | |
| | 5 | KJ-17 | | 1.87 | 2.85 |
| | 20 | KJ-14 | 79°F (26.11°C) | 1.989–2.28 | 1.56 |
| B | 35 | KJ-15 | 10% | 1.70 | 3.13 |
| | 50 | KJ-16 | | 2.63 | 2.34 |
| | 80 | KJ-18 | | | |
| | 5 | KJ-17 | | 2.35 | 2.74–3.13 |
| | 20 | KJ-14 | 116°F (46.67°C) | 2.0 | 1.82 |
| B | 35 | KJ-15 | 10% | 2.34 | 2.36 |
| | 50 | KJ-16 | | 1.66 | 2.73–2.80 |
| | 80 | KJ-18 | | | |

of energetic propellants is a function of AP modal distribution concentration and that propellants containing the larger AP particle sizes were more ESD sensitive.

From the inert samples, it appears that the major contributor to the dielectric field strength is the aluminum concentration.[18-20] The NaCl (total) concentration introduces second-order effects, while the fine NaCl has third-order effects. Attempts were made to break down pure HTPB binder and the measured dielectric strength was 23 MV/m.

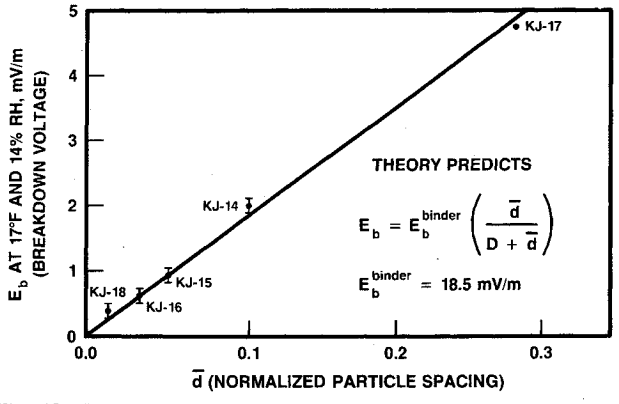


**Fig. 13 Breakdown voltage vs normalized particle spacing for the inert propellants. The straight line was determined by modeling and the specific data points are experimentally obtained.**

Table 6 summarizes the dielectric-breakdown data for propellants A and B. Neither propellant was temperature dependent, and the magnitude of the dielectric field strengths for both propellants were about the same. This result is not surprising since the two formulations are quite similar. The dielectric strength for propellant C at all temperatures was greater than the $9 \times 10^6$ V/m. The inability to measure the dielectric strength of propellant C is not surprising because insufficient metal-like species (ZrC) are present to cause the sample to break down.

Microstructural modeling of the electrical breakdown was performed by Beale and Larson of Electromagnetic Applications, Inc., Lakewood, Colorado,[21] using the formulation data in Table 1. The model calculated the spacing of the aluminum particles in the interstitial region. Figure 13 shows how the calculated spacing was used to plot the experimental breakdown voltage in Table 4. As shown, a good linear fit exists with the experimental data of the inert propellant formulations. The slope of the line is the breakdown field strength of the HTPB binder, which is 18 mV/m (about six times the free space value).

The breakdown voltage of the HTPB binder was measured to be 23 mV/m. This value is in very good agreement with the calculated value. Such good agreement between experimental results and the microscopic model derived by Beale and Larson[21] is excellent proof that the only influence of NaCl (or AP in real propellants) on the breakdown is its effect on the

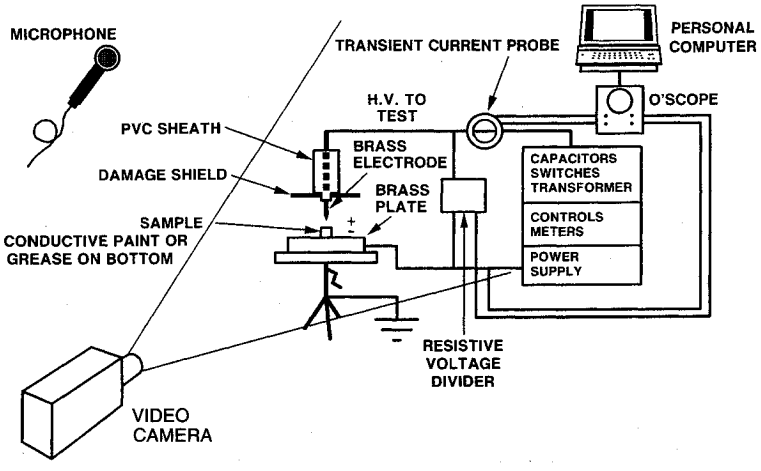


**Fig. 14 Schematic of the Naval Weapons Center electrostatic discharge R-C test apparatus modeled after the SNPE design.**

**Table 6 Dielectric-strength data for energetic propellants samples A and B**

| Method used | Electrode configuration | Temperature (RH[a] < 30%) | Dielectric strength × $10^6$ V/m 0.63-cm sample | 1.27-cm sample |
|---|---|---|---|---|
| | | Propellant A | | |
| Ramp | A | 40°F (4.44°C) | 0.75 | 0.85 |
| | | 70°F (21.11°C) | 1.12 | 1.25 |
| | | 90°F (32.22°C) | 0.78 | 0.94 |
| Switched capacitor | A | 95°F (35°C) | | 0.70–0.91 |
| | C | 95°F (35°C) | 0.70–0.94 | |
| | D | 95°F (35°C) | 0.67–1.06 | |
| Coil | A | 40°F (4.44°C) | 0.72 | |
| | | 70°F (21.11°C) | 0.64 | 0.48–0.53 |
| | | 95°F (35°C) | 0.73–0.74 | |
| | C | 95°F (35°C) | 0.76–0.86 | |
| | D | 95°F (35°C) | 0.98–1.12 | |
| | | Propellant B | | |
| | | 40°F (4.44°C) | 0.69 | 0.58 |
| Ramp | A | 70°F (21.11°C) | 0.62 | 0.66 |
| | | 95°F (35°C) | 0.69 | 0.62 |

[a]Relative humidity.

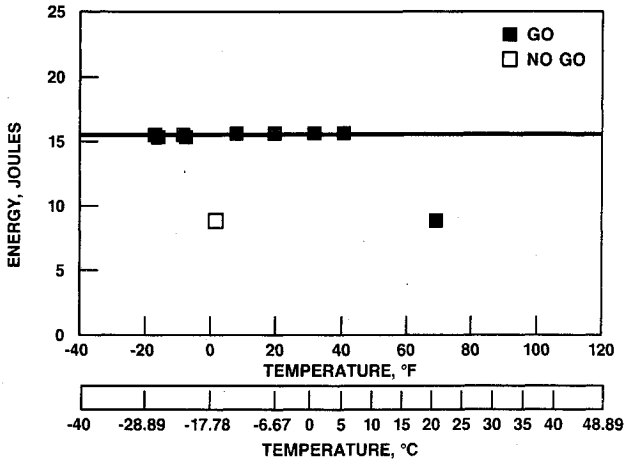


**Fig. 15 R-C discharge test results for model propellant A.**

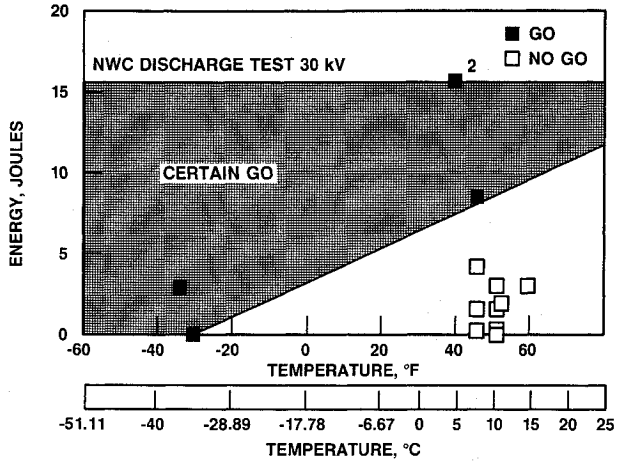


**Fig. 16 R-C discharge results for propellant B.**

spacing of the aluminum particles (i.e., NaCl has a geometrical effect only).

#### Step 5. R-C Discharge Test (Large Scale)

A variety of ESD R-C discharge tests have been developed and are described in Refs. 3 and 4. In the NWC logic/protocol, an R-C discharge test was incorporated because of its demonstrated utility in the Pershing II investigation. This test showed when the propellant would be sensitive to ESD events, particularly at the colder temperatures. Details of this R-C discharge test can be found in Ref. 8.

This ESD test uses an R-C discharge approach through representative propellant samples 9.0 cm in diameter and 10.0 cm long. "Go" or "no/go" results as a function of temperature and humidity can be obtained from such tests. The basic features of the R-C discharge test are:

1) A known energy is applied through a point brass electrode and allowed to dissipate through the propellant to a brass plate electrode.

2) A typical test series contains 30 consecutive discharges on each of three identical specimens at 15.6 J (30 kV and 34.7 nF).

If any of the 90 discharges results in cracking, popping, smoke, or fire, then the formulation is considered sensitive to ESD. Figure 14 shows the test setup for the NWC electrode static discharge test. Electrode contact to the propellant is ensured by slightly forcing the tip of the brass electrode approximately 1 mm into the propellant and by using conductive silver paint (E-Kote 40 silver conductive paint from Allied Products Corp.) between the plate electrode and the propellant. A voltage range of 0–45 kV, currents of up to 2.0 mA, and a maximum capacitance of 35 nF are available on this instrument. Energies up to 15.6 J can be discharged through the propellant.

Electrostatic discharge tests were performed on propellants A and B as a function of temperature and applied energy and the data are summarized in Figs. 15 and 16. These data show that both propellants are ESD sensitive. The sensitivity of propellant B also increases as the temperature decreases.

## Summary and Conclusions

The NWC ESD logic/protocol was applied to HTPB-based inert propellants to learn more about the mechanisms of ESD events. The protocol was also applied to energetic propellant formulations in an attempt to check predictions deduced from the inert propellants and to validate the logic/protocol with real propellants. Data taken on the inert propellant samples showed that the volume resistivity, dielectric constant, and dielectric strength are very sensitive to composition. The overall electrical properties of the materials are influenced by the HTPB binder and to a lesser extent by the concentration and particle size[18] of the aluminum (conducting) particles. The oxidizer (nonconducting) particles contribute only geometrically to influence the spacing of the aluminum particles.

All the electrical measurements (both on inert and energetic propellant samples) have empirically validated the percolation relationship. For example, in the percolation calculation, the binder influences the $P_{imp}$ value the most. This effect has been validated by ESD measurements performed on propellants with more conductive binders,[8,15] in which the ESD sensitivity of those systems is drastically reduced. These propellants tend to have low volume resistivity ($10^5$–$10^{10}$ Ω·cm; $10^3$–$10^8$ Ω·m), larger dielectric constants (10–300 at 1 kHz), and moderate-to-high dielectric-breakdown field strength ($\sim$1–6 $\times$ $10^6$ V/m).

From the percolation calculation, it is evident that the conducting particles (i.e., aluminum) also influence the ESD sensitivity. Data obtained in this study show that, for HTPB-propellant systems, the aluminum dramatically influences the electrical properties of the overall propellants. For example, the dialectric constant of the inert samples is proportional to the aluminum volume percent. The larger the dielectric constant, the more energy can be stored, and thus the material is more ESD sensitive. Therefore, it is desirable to have large dielectric constants in HTPB propellants. The dielectric-breakdown strength of the inert propellants shows decreasing strength with increasing volume percent of aluminum. It has also been shown[18] that decreasing the particle size of the aluminum increases the dielectric-breakdown strength. These experimental results were found to be in good agreement with microstructural modeling of electrical breakdown in solid fuel propellants provided by Beale and Larson.[21] From this result, it can be concluded that HTPB propellants can be made more ESD safe if the aluminum (conducting particle) concentration is reduced (below 20 vol%), or the aluminum particle size is reduced. This conclusion is confirmed in energetic propellants. Propellant C is less ESD sensitive than propellants A or B because it contains only small amounts (1–4%) of conducting particles. Furthermore, propellant B appears to be more reactive than propellant A in the R-C discharge experiment because it contains slightly larger aluminum particles.

The contribution to ESD sensitivity of the nonconducting particles is also seen in these experimental results. The dielectric strength for the inert propellant formulations increases as the NaCl concentration increases. Therefore, to make ESD-safer propellants, the solids loading of the nonconducting particles should be increased. This approach would minimize the contribution of the binder to the electrical properties. The dielectric strength also increases as the concentration of fine NaCl increases. It was also found by Berger et al.[22] that in propellant formulations that have more of the fine nonconducting particles, the breakdown voltage is significantly increased. This increase would imply that formulations having finer particle-size distributions of the nonconducting particles tend to be less ESD sensitive. The distribution should have a

greater concentration of fine oxidizer particles; however, such a formulation change may significantly alter the performance of the propellant. This conclusion is supported by the data presented on the energetic propellant formulations. Propellant C has a larger AP solids loading compared to propellant A or B; thus data show that propellant C is better behaved in an ESD environment. Furthermore, propellant A has a larger concentration of fine AP compared to propellant B, and the R-C discharge data show propellant A to be less sensitive, particularly at the colder temperatures.

In conclusion, the HTPB class of propellants should be modified as follows to make them less susceptible to ESD events:

1) Change the HTPB binder to a more conductive type.

2) Reduce the concentration of conducting particles to less than 20 vol%.

3) Decrease the particle size of the conducting particles and make them more uniform.

4) Increase the solids loading and broaden the modal distribution of the nonconducting particles. This increase should be made in such a manner that the conducting particle packing allows the particles to be as far from each other as possible.

5) Add trace concentrations of conducting species.

Such formulation changes would allow the electrical properties to be modified as follows:

1) The resistivity of the propellants would be lowered.

2) The dielectric constant would be reduced and the dissipation factor would be increased.

3) The dielectric strength should be large so that the breakdown cannot readily be reached under normal operating procedures.

4) The ignition energy (i.e., that energy required for a sustained ignition to exist) should be relatively high in order to ensure that no ignition can take place during normal handling of the rocket motors.

The electrical phenomena addressed in the logic/protocol are all interrelated. A technology has been developed that allows the investigation and ranking of ESD sensitivity in propellants, and suggests methods to mitigate concerns. However, further work is still required in understanding the mechanism of ESD-triggered events. Before the above suggested propellant changes are made and the propellant is qualified to be used in a solid rocket motor, the ESD sensitivity should be re-evaluated on the revised formulation.

## Acknowledgments

The authors would like to thank Phil W. Gibson, formerly of the Air Force Astronautics Laboratory, Edwards AFB, California, for providing the inert propellants. Sincere appreciation is also extended to Ronald W. Larson and Paul D. Beale for their helpful discussions and contributions in the modeling of the breakdown field strength.

## References

[1]Mardikguian, M., *Electrostatic Discharge—Understand, Simulate and Fix ESD Problems,* Interference Control Technologies Inc., Gainesville, VA, 1985, p. vi of Preface.

[2]Knauer, J. A. (ed.), *Technical Investigation of 11 January 1985 Pershing II Motor Fire,* U.S. Army Missile Command, TR RK-85-9, Vol. III A, Dec. 31, 1985.

[3]Brown, F. W., Kusler, D. J., and Gibson, F. C., *Sensitivity of Explosives to Initiation by Electrostatic Discharges,* Bureau of Mines Rept. of Investigations 5002, Sept. 1953.

[4]Kent, R., and Rat, R. J., "Static Electricity Phenomena in the Manufacture and Handling of Solid Propellants," *Journal of Electrostatics,* Vol. 17, No. 299, 1985, pp. 299–312.

[5]Hammersley, J. M., and Hanscomb, D. C., *Monte Carlo Methods,* Spottiswoode, Ballentyne and Co., London, UK, 1964, pp. 134–141.

[6]Hammersley, J. M., and Broadbent, S. R., "Percolation Process—I. Crystals and Mazes," *Proceedings of the Cambridge Philosophical Society,* Vol. 53, 1957, pp. 629–641.

[7]Frisch, H. L., and Hammersley, J. M., "Percolation Processes and Related Topics," *Journal of the Society for Industrial and Applied Math,* Vol. 11, Dec. 1963, pp. 894–918.

[8]Covino, J., *Electrostatic Discharge (ESD) Sensitivity of a Selected Number of Solid Rocket Propellants,* Chemical Propulsion Information Agency, Johns Hopkins Univ. Applied Physics Lab., Laurel, MD, CPIA Pub. 464, Vol. 1, March 1987, p. 335.

[9]Keithley Instruments, Inc., *Low Level Measurement for Effective Low Current, Low Voltage, and High Impedance Measurements,* 3rd ed., Cleveland, OH, 1984, pp. 63–66.

[10]American Society for Testing and Materials, "Standard Test Methods for D-C Resistance of Conductance and Insulating Materials," *ASTM Standard D257-78,* reapproved 1983.

[11]Berger, M. A., Losee, L. A., and Speed, T. C., "Effect of Measuring Parameters on the Volume Resistivity and Dielectric Constant of Solid Rocket Propellants," *Proceedings of the 1987 JANNAF Propulsion Systems Hazards Meeting,* Chemical Propulsion Information Agency, Johns Hopkins Univ. Applied Physics Lab., Laurel, MD, CPIA Pub. 464, p. 287.

[12]Smyth, C. P., *International Chemical Series Dielectric Behavior and Structure,* McGraw-Hill, New York, 1955.

[13]West, A. R., *Solid-State Chemistry and its Applications,* Wiley, New York, 1984, pp. 534–540.

[14]American Society for Testing Materials, "Standard Methods of Test for A-C Loss Characteristics and Dielectric Constant (Permitivity) of Solid Electrical Insulating Materials," *ASTM Standard D150-70* (Annual Book of ASTM Standards by American Society for Testing and Materials), 1971, p. 27.

[15]Covino, J., and Hudson, F. E., III, "The Measurement of Dielectric Constants for Propellants and Propellant Ingredients," *Proceedings of the 1987 JANNAF Propulsion Systems Hazards Meeting,* Chemical Propulsion Information Agency, Johns Hopkins Univ. Applied Physics Lab., Laurel, MD, CPIA Pub. 464, p. 277.

[16]American Society for Testing Materials, "Standard Test Method for Dielectric Breakdown Voltage and Dielectric Strength of Solid Electrical Insulating Materials at Commercial Power Frequencies," *ASTM Standard D149-81,* 1981, pp. 1–13.

[17]IEEE Standard Techniques for High-Voltage Testing, 16th ed., *IEEE Standard 4-1969,* pp. 37–125.

[18]Covino, J., and Hudson, F. E., III, "Dielectric-Breakdown and Dielectric-Strength Measurements for Propellants and Propellant Ingredients," *Proceedings of the 1987 JANNAF Propulsion Meeting,* San Diego, CA, Dec. 1987 (to be published).

[19]Speed, T. C., Losee, L. A., and Berger, M. A., "Dielectric Breakdown of Rocket Motor Propellants—Methods, Analysis, and Data," *Proceedings of the 1987 JANNAF Propulsion Systems Hazards Meeting,* Chemical Propulsion Information Agency, Johns Hopkins Univ. Applied Physics Lab., Laurel, MD, CPIA Pub. 464, p. 303.

[20]Gibson, P. W., and Benedict, R. E., "Effects of Formulation on the Electrostatic Sensitivity of Solid Rocket Propellants," *Proceedings of the 1987 JANNAF Propulsion Systems Hazards Meeting,* Chemical Propulsion Information Agency, Johns Hopkins Univ. Applied Physics Lab., Laurel, MD, CPIA Pub. 464, p. 371.

[21]Beale, P. D., and Larson, R. W., "Microstructural Modeling of Electrical Breakdown in Solid Fuel Propellants," *Proceedings of the Workshop on ESD Ignition of Composite Solid Propellants,* Nashville, TN, April 1989.

[22]Berger, M., Brown, M. J., Dollmeyer, E. L., and Speed, T. C., "Effect of Al and AP Size Variations on Propellant Dielectric Breakdown," *Proceedings of the 1989 JANNAF Propulsion Systems Hazards Subcommittee Meeting,* Chemical Propulsion Information Agency, Johns Hopkins Univ. Applied Physics Lab., Laurel, MD, CPIA Pub. 509, Vol. 1, 1989, pp. 241–253.